

# When a Black Hole Winks...

... in a galaxy far, far away...

- Author: Shyeh Tjing Cleo Loi (October 2010)

A supermassive black hole millions of times the mass of our sun is believed to reside within the heart of every galaxy - an object with such an intense gravitational field that nothing, not even light, can escape. By that definition alone, one would be inclined to think that there is perhaps more to a black hole than meets the eye. And so we turn our radio telescopes to the heavens, and observe with a fresh pair – or six.



Figure 1. Photograph of the Australia Telescope Compact Array (image credit: ATNF website)

The Australia Telescope Compact Array (ATCA), located in Narrabri and operated by a CSIRO division called the Australia Telescope National Facility (ATNF), makes use of six 22-metre movable antennae (five of which are shown in Fig. 1) to observe the radio sky. Spread over 6 kilometers, the array uses the technique of aperture synthesis, a class of interferometry, to increase telescope resolution. The array has the ability to map the fine radio structure of distant objects, offering valuable insight into the formation and

evolution of extended structures whipped up around *active galactic nuclei* (AGN) during intermittent episodes of violent activity.

AGN are compact regions typically less than 1 kiloparsec across at the centres of galaxies which produce immense amounts of energy over most of the electromagnetic (EM) spectrum. Galaxies which host radio-loud AGN comprise a small fraction (~0.01%) of all known galaxies, and are almost exclusively giant ellipticals, many of which are located at the centre of galaxy clusters. These are termed *radio galaxies*.

The energetic outbursts of AGN are thought to occur during periods when the central black hole has had – simply speaking - too much to eat. A massive and prolonged cosmic burp sees the production of megaparsec-scale jets and/or lobes (see Fig. 3), the eventual dimensions of which usually dwarf the host radio galaxy itself. The nuclear regions and the structures ploughing their way through the intergalactic medium (IGM) are prominent radio-frequency emitters, the spectra of which are believed to be shaped by the interplay of the following non-thermal processes:

### *Synchrotron emission*

- the radiation emitted by charged relativistic particles accelerated by magnetic fields; this arises in jets of what is thought to be pair plasma (electron-positron pairs) interacting with twisted field lines of the central object, and ionised gas swirling around the active core

*Synchrotron self-absorption*

- the opposite process to synchrotron emission, where radio photons are re-absorbed by plasma particles

**$1 \text{ Jy} = 10^{-26} \text{ W m}^{-2} \text{ Hz}^{-1}$**   
 Jansky - a unit of EM flux density (energy per surface area) named after the pioneering radio astronomer, Karl Jansky

An important clue to the nature of AGN core activity is the timescale over which it acts. Determining this is slightly tricky, however. If we know the speed of the jets and the true size of the structures, we can work out how old they are. Sounds simple, but if we don't know how these structures are angled in the sky or whether the jet speed changes over time, our estimation could be considerably off-the-mark. Interestingly enough, however, the age of the core can be determined from its *radio spectrum* (a graph of intensity against frequency). If the spectrum shows a peak (such as in Fig. 2), we can work out its age by identifying the frequency of that peak. These are related through a 'Youth Scenario' - the younger the source, the higher the peak frequency.

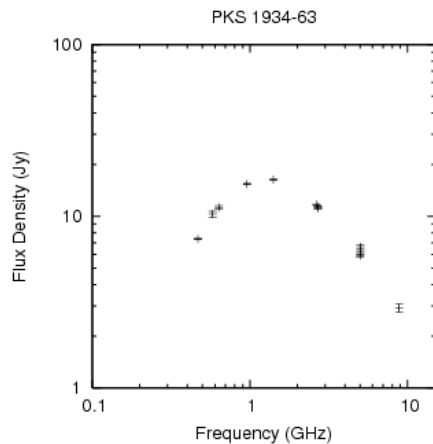


Figure 2. Spectrum of GPS source PKS 1934-63

*Gigahertz-peaked spectrum* (GPS) sources are a class of objects which have a spectral peak in the gigahertz

range ( $\geq 1 \text{ GHz}$ ), and these are believed to host the very youngest of AGN.

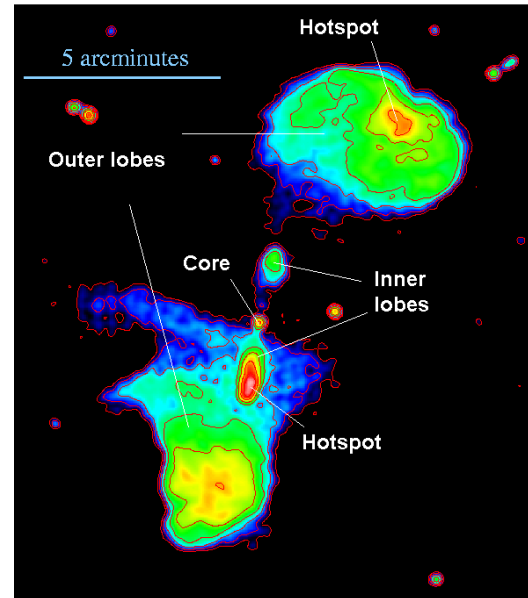


Figure 3. Giant radio galaxy J0116-473 showing both a pair of outer and inner lobes, thought to form from the stopping and restarting of central activity. The colours represent different intensities of radio emission. (20 cm wavelength ATCA image by Saripalli et al. 2002)

Radio frequencies range from  
 **$\sim 30 \text{ kHz} - 300 \text{ GHz}$**   
 with corresponding wavelengths ranging from  
 **$\sim 1 \text{ mm} - 10 \text{ km}$**

*The Australia Telescope 20 Gigahertz Survey (AT20G)*

In a recent blind survey completed by ATCA in 2008, the whole of the southern sky was mapped out at 20GHz, with nearly simultaneous follow-up measurements at 8.6 and 4.8 GHz. This survey, known as the *Australia Telescope 20 GHz survey* (AT20G for short), is one of the first of its scale and sensitivity to make high-frequency ( $>5 \text{ GHz}$ ) observations of extragalactic objects (Murphy et al. 2010). Flux densities above a threshold of 40 mJy, polarisation measurements and positions of a total of 5890 sources are currently listed in the survey catalogue, with 3795 of these having a measured flux at all three frequencies.

## Scouring the inky depths of space

While a large number of double-lobed radio galaxies are known, a small subset of these possess a set of inner lobes in addition to the outer pair (such as J0116-473 in Fig. 3) which appear to form due to intermittent periods of central activity. These are termed *double-double radio galaxies* (DDRGs), which can be considered a type of *restarted radio galaxy*: one which is partway through its second epoch of activity. However younger still are those that have only just begun their second stage of activity but whose inner structure cannot yet be resolved (made clearly visible).

The aim of this project was to detect galaxies with dying lobes and with a core at its critical point of rebirth – *the youngest restarted galaxies*. These would have two important features:

1. A *twin-lobed structure* in their radio image (from a previous round of activity)
2. A *high-frequency peak* in their radio spectrum (produced by new core emission)

The shape of a radio spectrum can be described by a power law, with the flux at a particular frequency characterised by a spectral index:

$$S \propto \nu^\alpha$$

where  $S$  denotes flux,  $\nu$  denotes frequency and  $\alpha$  is the spectral index. The spectral index represents the slope of the spectral graph when this is plotted on logarithmic axes. Sources in the AT20G catalogue were grouped according to their average spectral index over two frequency bands, and a ‘two-colour’ plot was produced (Fig. 4).

GPS sources were selected as being the ones which had a rising spectrum over the lower frequency band ( $\alpha_{4.8}^{8.6} \geq 0.2$ ), yielding a sample of 789. This selection method included sources with and without an observed peak below 20 GHz. It was assumed that the sources which had a spectrum which rose over the measured range (described as ‘inverted’) would peak and turn over eventually at frequencies in excess of 20 GHz. This has been found to be the case

### Spectral Indices at Two Frequency Bands

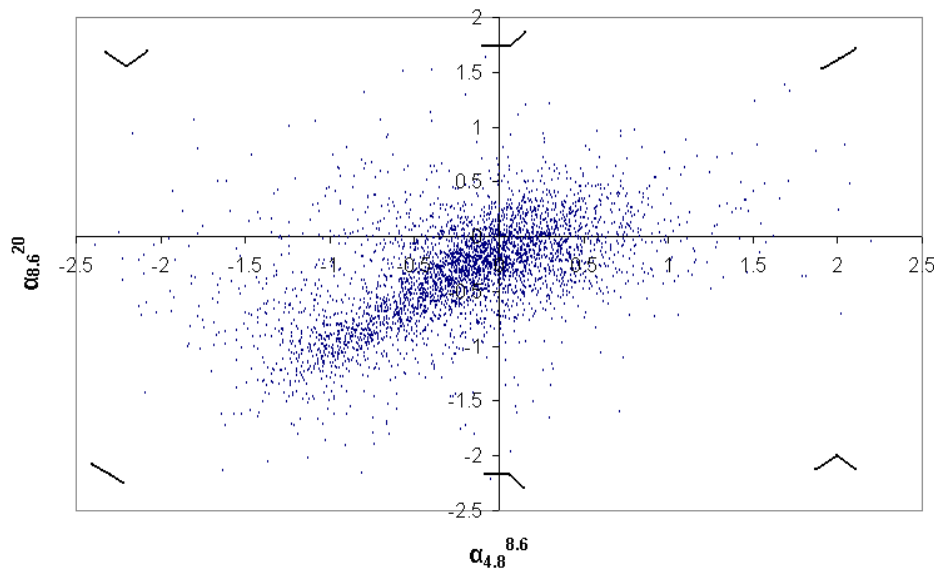


Figure 4. Plot showing spectral index distribution for 3795 sources in the AT20G survey. On the x-axis is the average spectral index from 4.8 to 8.6 GHz and on the y-axis is that from 8.6 to 20 GHz. In most sources there is minimal difference between the two values.

in a study by Sadler et al. (2008), where almost all sources in a sample from the AT20G with inverted spectra at 8-20 GHz were found to have peaked by 95 GHz.

The definition of *redshift* (symbol  $z$ ):

$$z = \frac{\Delta\lambda}{\lambda}$$

where  $\Delta\lambda$  is the measured shift in wavelength with respect to rest-frame wavelength  $\lambda$

### *Navigating the skies with contour maps*

*Contour maps* showing flux density levels at 843 MHz and 1.4 GHz of the 789 sources were generated from their low-frequency radio images. In a long and painstaking effort, each of the 789 images was individually examined for the presence of an extended structure. This was paid off by the discovery of just 36 such objects, 11 of which were double-lobed.

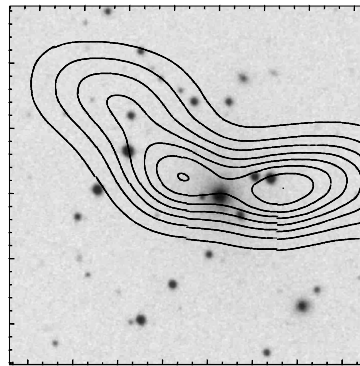
In order to determine the effectiveness of this method in finding double-lobed radio sources among those with a GPS core, a random sample of 203 from the original 5890 was taken and their contour plots inspected. Of these, 9 were extended in some way and 4 had a double structure. The success rate for finding double-lobed sources in both the random and GPS samples was thus very similar, on the order of ~1-2%. This suggests that galaxies at any stage of their lives are just as likely to possess a twin-lobed structure.

## *Seeing Double*

Out of the 11 double-lobed sources with GPS cores found by this method, only 4 had been previously identified as such. The 7 other sources therefore represent

### *What are contour maps?*

Plots which have lines joining up regions of equal electromagnetic flux density are known as *contour maps*. Just like a topographic map showing the relief of a landscape, these plots show the shape and structure of radio emission produced by a distant object. Below is an example of such a plot overlaid onto the optical image of source J062648-543214, showing a complicated structure that has multiple bright regions.



a *newly-identified* sample of restarted radio galaxies. These 11 are as follows, with the new sources in **boldface**:

J005427-341949  
 J010333-643907  
**J023137-204021**  
**J043022-613201**  
 J074619-570258  
**J133639-335756**  
**J134928-704847**  
**J161421-370503**  
 J181857-550815  
**J223040-394252**  
**J225336-345529**

Using redshift data from the 6dF Galaxy Survey (6dFGS) (Jones et al. 2004), radio data from the Sydney University Molonglo Sky Survey (SUMSS) (Mauch et al. 2003), NRAO/VLA Sky Survey (NVSS) (Condon et al. 1998) and the AT20G survey, and optical data from the SuperCOSMOS Sky Survey (SSS) (Hambly et al. 2001), lower limits for the size of extended structures were computed, as well as the minimum duration of interrupted activity.

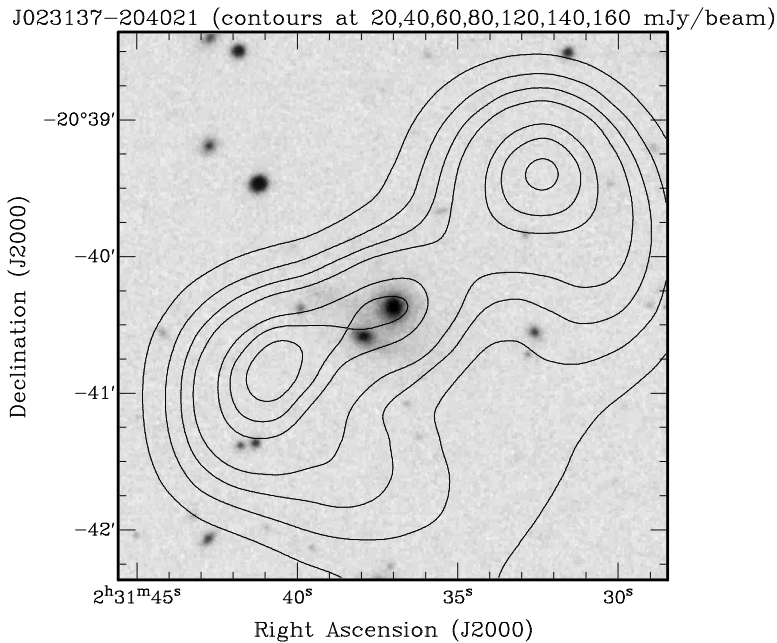


*Figure 5. Blue optical SuperCOSMOS image overlaid with 1.4 GHz NVSS contours for source J023137-204021. The optical image reveals a likely galaxy interaction, as the two galaxies in the centre of the image are found to have very similar redshifts ( $|\Delta z| < 0.001$ ) and are hence likely to be within gravitational influence of one another. [For images and data for all sources in the sample, please refer to the appendix.]*

With the exception of 3 sources (J181857-550815, J134928-704847 and J161421-370503) which had no SSS optical identification, the remaining 8 sources were listed as galaxies within the SuperCOSMOS database. Of these, the sources J010333-643907 and J223040-394252 were also classified in the NASA/IPAC Extragalactic Database (NED) as quasi-stellar objects (QSOs). Compare this to the proportions as found by Sadler et al. (2006) in the full AT20G sample – 65% QSOs and 25% galaxies - and you can see that double-lobed objects are far more likely to be galaxies rather than QSOs.

Table 2 summarises the minimum lower bounds for the timescale of halted activity in each of the 11 restarted galaxies. This value, expressed in millions of years, was obtained by assuming that the jet continues to propagate at very close to the speed of light, continuing to fuel the hotspot until it passes completely into it, at which point the lobes gradually begin to fade. And so the point where the last of the material has just stopped reaching

### **Galaxies vs. Quasars**

Quasars (short for quasi-stellar objects) are the most luminous objects in the universe, some estimated to be hundreds of times more luminous than the total light of an average galaxy. They appear as point-like stellar objects which are typically found at high redshifts, meaning they are extremely distant. Originally they were considered a separate type of object to galaxies, and controversy raged for many years as to the origin of their immense power. However the initial luminosity estimations assumed that the quasars were radiating uniformly in all directions, an assumption which is now believed to be false. Our modern understanding of quasars is that their power originates in an active galactic nucleus within a distant galaxy, and that in the case of radio-loud quasars we are looking down the intense collimated beam of radiation that produces lobes and jets in otherwise normal radio galaxies, when these are viewed side-on (Antonucci 1993).

the lobes, the time in years elapsed since the core ‘switched off’ would simply be the light-travel time across the structure. Inspection of the AT20G contour images revealed no high-frequency emission within the lobes with the exception of the inverted-spectrum source J181857-550815 (see Fig. 6). This still had residual 4.8 GHz emission in one lobe, suggesting that it had only recently stopped receiving power from the jet. The duration of halted activity quoted for this source should therefore be a somewhat closer approximation to the true value than those for the other sources in Table 2, where they otherwise represent strict lower-bound estimates.

Angular-size distances were obtained from the published redshift, using the values  $H_0 = 71 \text{ km s}^{-1} \text{ Mpc}^{-1}$ ,  $\Omega_M = 0.27$  and  $\Omega_{vac} = 0.73$  and the algorithm provided by Ned Wright’s Cosmology Calculator (Wright 2006). These and the measured angular sizes then yielded the projected linear size.

### ***The Cosmological Parameters***

Hubble’s constant ( $H_0$ ) is a measure of the recession velocity of an astronomical object at a certain distance. It has a non-zero value which reflects the fact that the universe is expanding, and that objects further away are moving faster from us.  $H_0$  is believed to change over time, with its current measured value estimated to be about 71 kilometers per second per megaparsec.

The density parameters,  $\Omega_M$  and  $\Omega_{vac}$ , denote the ratio of matter density and vacuum energy density respectively to the critical density of the universe (the density required to just stop the universe expanding forever). Combinations of these values result in various geometries, or curvatures, of spacetime. For this reason these two parameters must be taken into account when calculating angular sizes or luminosities of distant galaxies or quasars from their redshift.

*Table 2. Summary of data on 11 restarted galaxies.*

<b>Source name</b>	<b>Redshift</b>	<b>Angular size (arcmin)</b>	<b>Projected size (kpc)</b>	<b>Duration of interruption (Myr)</b>
J005427-341949	0.1103	2.8	330	0.54
J010333-643907	0.163	2.8	470	0.76
J023137-204021*	0.089838	2.4	240	0.39
J043022-613201*	0.055498	2.0	130	0.21
J074618-570258	0.13	0.51	70	0.11
J133639-335756*	0.0124	1.9	29	0.046
J134928-704847*		1.4		
J161421-370503*		2.4		
J181857-550815	0.072634	1.5	120	0.20
J223040-394252*	0.318049	3.3	910	1.5
J225336-345529*	0.2115	4.6	940	1.5

\* indicates a newly-identified restarted galaxy

It was noted that another source (J031552-190644) which was coincident with an edge-on spiral galaxy and appeared to have a partially-resolved bipolar elongation, had been subject to prior study by Ledlow et al. (1998) who describe it as an FR I radio source having ‘a pair of nearly

symmetrical lobes of total extent ~200 kpc’. It is therefore important to realise that there could very well be additional double-lobed galaxies within the extended sample of 36 that have not been resolved in the 843 MHz and 1.4 GHz surveys, as this formed the basis of identification.

J181857-550815 (0.8 GHz contours at 20,40,80,120,160,200,240,280,320 mJy/beam)

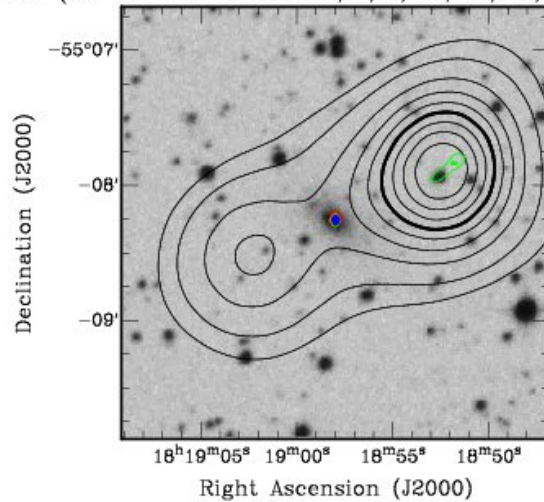


Figure 6. Blue optical SSS image overlaid with 843 MHz SUMSS radio contours, with AT20G contours in red (20 GHz), blue (8.6 GHz) and green (4.8 GHz)

## Conclusions and Future Work

Flux data from the AT20G survey has enabled the identification of 7 previously unknown restarted double-lobed radio galaxies. The success rate of finding double-lobed galaxies in the AT20G sample was of order 1-2%, and this appeared not to vary between galaxies with different core ages. It is possible that there are still more restarted galaxies to be found whose lobes have not been resolved, or perhaps were too faint to be detected within SUMSS or NVSS.

To all young aspiring radio astronomers who happen to cast more than a nanosecond-long glance across these words, you may be pleased to hear that there is no limit, theoretical, philosophical or otherwise, to the future work that needs to be done. The most immediate tasks are to obtain a redshift value for J134928-704847 and J161421-370503, conduct VLBI (Very Long Baseline Interferometry) observations in order to place tighter upper estimates on the core diameters, and to resolve any double structure in the remaining sources of the extended

GPS sample. Additional flux data for the core and lobes of each source would enable the construction of a more reliable radio spectrum and hence offer greater accuracy in determining the age of each component. Greater sensitivity measurements could reveal fainter structures than were able to be reliably identified in the aforementioned surveys, and this could assist in the identification of more restarted radio galaxies.

At this point we have estimated the timescales of nuclear interruptions to be on the order of fractions of a million years – vanishingly brief moments in the lifetime of an average galaxy. But until we can claim we understand these duty cycles of activity in young active galactic nuclei, the formation and evolution of these strange cosmic objects will remain a mystery – locked in the innocent wink of a black hole's eye.

## *Acknowledgements*

This research has made use of the NASA/IPAC Extragalactic Database (NED) operated by the Jet Propulsion Laboratory, California Institute of Technology, under contract with the National Aeronautics and Space Administration.

I would like to thank TSP coordinators Dick Hunstead and Mike Biercuk for the opportunity to be involved in this work, and my parents and brother for their technical support. Last but not least I would like to thank my project supervisor, Paul Hancock, for his patient advice, words of wisdom and the leery eye he has been keeping over my shoulder.

## *References*

- Antonucci, R., 1993, A&A, 31, 473  
Condon, J.J. et al. 1998, AJ, 115, 1693  
Hambly, N.C. et al. 2001, MNRAS, 326, 1279  
Jones et al. 2004 MNRAS 355, 747  
Ledlow, M.J. et al. 1998, ApJ, 495, 227  
Mauch T., Murphy T., Buttery H.J., Curran J., Hunstead R.W., Piestrzynska B., Robertson J.G. and Sadler E.M. 2003, MNRAS, 342, 1117  
Murphy, T. et al., 2010, MNRAS, 402, 2403  
Sadler, E.M. et al. 2006, MNRAS 371, 898  
Sadler et al. 2008, MNRAS, 385, 1656  
Saripalli, L., Subrahmanyam, R., Shankar, N.U. 2002, ApJ 565:256  
Wright 2006, PASP, 118, 1711  
Hancock, P.J. et al. 2009, MNRAS, 397, 2030  
Kaiser, C. R., Schoenmakers, A. P. and Röttgering, H. J. A. 2000 MNRAS 315: 381  
Peterson, B. M. 1997, An Introduction to Active Galactic Nuclei, Cambridge Univ. Press, Cambridge  
Tzioumis, A. et al. 2002, A&A 392 (3) 841

## *Bibliography*

- Bowers, R.L. 1972 Phys. Rev. Lett. 29, 509  
Hancock, P.J. 2009, AN 999, No.88, 789